HHS Public Access

Author manuscript

Circ Heart Fail. Author manuscript; available in PMC 2022 February 01.

Published in final edited form as:

Circ Heart Fail. 2021 February ; 14(2): e007279. doi:10.1161/CIRCHEARTFAILURE.120.007279.

Mineralocorticoid Receptor in Smooth Muscle Contributes to Pressure Overload-Induced Heart Failure

Seung Kyum Kim, PhD[1,2], **Lauren A. Biwer, PhD**[1], **M. Elizabeth Moss, BA**[1,3], **Joshua J. Man, BS**[1,3], **Mark J. Aronovitz, MS**[1], **Gregory L. Martin, BS**[1], **Francisco J. Carrillo-Salinas, PhD**[4], **Ane M. Salvador, PhD**[4], **Pilar Alcaide, PhD**[4], **Iris Z. Jaffe, MD, PhD**[1,*]

[1]Molecular Cardiology Research Institute, Tufts Medical Center, Boston, MA

[2]Department of Sports Science, Seoul National University of Science and Technology, Seoul, Republic of Korea

[3]Graduate School of Biomedical Sciences, Tufts University School of Medicine, Boston, MA

[4]Department of Immunology, Tufts University School of Medicine, Boston, MA

Abstract

Background: Mineralocorticoid receptor (MR) antagonists decrease heart failure (HF) hospitalization and mortality but the mechanisms are unknown. Preclinical studies reveal that the benefits on cardiac remodeling and dysfunction are not completely explained by inhibition of MR in cardiomyocytes, fibroblasts or endothelial cells. The role of MR in smooth muscle cells (SMC) in HF has never been explored.

Methods: Male mice with inducible deletion of MR from SMCs (SMC-MR-KO) and their MR-intact littermates were exposed to HF induced by 27-gauge transverse aortic constriction (TAC) versus sham surgery. HF phenotypes and mechanisms were measured four weeks later using cardiac ultrasound, intracardiac pressure measurements, exercise testing, histology, cardiac gene expression, and leukocyte flow cytometry.

Results: Deletion of MR from SMC attenuated TAC-induced HF with statistically significant improvements in ejection fraction, cardiac stiffness, chamber dimensions, intracardiac pressure, pulmonary edema and exercise capacity. Mechanistically, SMC-MR-KO protected from adverse cardiac remodeling as evidenced by decreased cardiomyocyte hypertrophy and fetal gene expression, interstitial and perivascular fibrosis, and inflammatory and fibrotic gene expression. Exposure to pressure overload resulted in a statistically significant decline in cardiac capillary density and coronary flow reserve in MR-intact mice. These vascular parameters were improved in SMC-MR-KO mice compared to MR-intact littermates exposed to TAC.

Conclusion: These results provide a novel paradigm by which MR inhibition may be beneficial in HF by blocking MR in SMC thereby improving cardiac blood supply in the setting of pressure

[*]Correspondence to: Iris Z. Jaffe, MD, PhD, Molecular Cardiology Research Institute, Tufts Medical Center, 800 Washington Street, Boston, Massachusetts, 02111. Fax: 617-636-1444; Tel: 617-636-0620; ijaffe@tuftsmedicalcenter.org.

Disclosures: none

overload-induced hypertrophy thereby mitigating the adverse cardiac remodeling that contributes to HF progression and symptoms.

Journal Subject Terms:

ACE/Angiotensin Receptors/Renin Angiotensin System; fibrosis; hypertrophy; remodeling; heart failure; animal models of human disease; basic science research; coronary circulation

Introduction

Ample clinical data support a role for the mineralocorticoid receptor (MR) in heart failure (HF) pathophysiology. Multiple randomized trials demonstrate that MR inhibition decreases mortality from HF with reduced ejection fraction (HFrEF) and prevents HF hospitalization in patients with HFrEF or HF with preserved ejection fraction (HFpEF).[1-5] Much of the cardiac benefit of MR antagonism is independent from MR inhibition in the kidney.[6] Indeed, a meta-analysis of MR antagonist trials showed that patients randomized to MR inhibition had improved ejection fraction (EF), decreased LV volume, decreased circulating fibrosis markers and improved diastolic function, indicating direct beneficial effects on cardiac remodeling.[7] The MR is expressed throughout the heart including in cardiomyocytes, fibroblasts, endothelial cells (EC) and smooth muscle cells (SMC). However, the cell type-specific mechanisms for the benefits of MR inhibition on cardiac remodeling remain incompletely understood.

Benefits of MR antagonism are also evident in preclinical studies using animal HF models. One commonly used mouse model of HF is transverse aortic constriction (TAC), where a permanent constriction is placed around the proximal aorta to induce LV pressure overload. The cardiac response begins with pathological hypertrophy and progresses to chamber dilation and decreased systolic function.[8] With severe TAC, this leads to pulmonary edema and ultimately death. Thus, TAC-induced pressure overload simulates aspects of pathological cardiac hypertrophy and progression to dilated cardiomyopathy as observed in patients with HF induced by hypertension, some valvular heart diseases, and even myocardial infarction. The pathophysiology involves cardiac hypertrophy, inflammation and ultimately fibrosis.[9, 10] In mice subjected to TAC, MR inhibition attenuates cardiac hypertrophy[11, 12], LV dilation[13], systolic dysfunction[12, 13], cardiac fibrosis[13], pulmonary edema and mortality.[13] Interestingly, while MR deletion in cardiomyocytes or ECs attenuated the decline in systolic function, there was no effect on cardiac hypertrophy, fibrosis, or inflammation.[14, 15] Furthermore, fibroblast MR deletion did not change the progression of HF.[14] Thus, it is likely that MR inhibition in cells other than cardiomyocytes, fibroblasts, or ECs mediates much of the benefit of MR antagonism.[16]

MR is expressed in vascular SMC and functions as a transcription factor to regulate SMC gene expression and function.[17-20] However, the role of SMC-MR in HF has never been tested. Thus, we exposed mice with inducible deletion of SMC-MR (SMC-MR-KO) to TAC versus sham surgery and compared the response to MR-intact littermates. We find that SMC-MR KO attenuates TAC-induced cardiac hypertrophy, fibrosis, stiffness, systolic dysfunction, and pulmonary edema and improves exercise capacity. Mechanistically, SMC-

MR deletion modulates mRNA expression of cardiac remodeling genes, prevents the decline in cardiac capillary density and improves coronary flow reserve (CFR). The results provide a novel paradigm for how MR inhibition may be beneficial in HF by blocking SMC MR activity and improving blood supply in the setting of pressure overload to attenuate adverse cardiac remodeling that contributes to poor HF outcomes.

Methods:

Detailed methods are available in Supplemental Material.

The data supporting this study are available from the corresponding author upon reasonable request.

Animals

Male SMC-MR-intact or SMC-MR-KO littermates were used at three months of age and all procedures were approved by the Tufts Institutional Animal Care and Use Committee. SMC-specific and inducible deletion of the MR has been previously confirmed in this model with no Cre recombinase activity in cardiomyocytes and no change in renal MR function after SMC-MR recombination.[20]

Transverse Aortic Constriction (TAC) surgery

Pressure overload-induced HF was produced by constricting the proximal aorta just after the first great vessel, as described previously.[8] Mice were randomized to severe (27G needle) TAC or sham operation and recovered for 4 weeks.

Non-invasive imaging and echocardiography

Echocardiography, pulse wave velocity and CFR measurements were conducted using Doppler ultrasound (Vevo 2100, VisualSonics). Cardiac functional parameters were assessed prior to TAC (Supplemental Table 1) and 4 weeks after TAC as described previously.[19, 21]

In vivo invasive hemodynamics

Four weeks after TAC, LV function was determined by invasive pressure-volume (PV) loop analysis in a subset of mice as described.[19]

Endurance exercise test

Endurance exercise capacity was determined by measuring run to exhaustion time normalized to body mass and vertical distance on the treadmill as described.[19]

Terminal tissue harvest

Serum was collected and aldosterone levels measured by radioimmunoassay as described.[19] Excised lungs were weighed immediately and after 48 hours ; the weight difference was quantified as pulmonary edema.[22] Left tibia length was used to normalize LV (+septum) weight to animal size.

LV Histological Analyses

One of two mid-papillary regions of LV tissues was formalin fixed, paraffin embedded, and sectioned at 5μm thickness. Sections were stained with Picrosirius Red (for fibrosis) and hematoxylin and eosin (for cardiomyocyte size). The other region was embedded in optimal cutting temperature compound and frozen. Cryosections were stained with anti-mouse CD31 (M1/70) to identify EC and LV capillary density was quantified as capillary area normalized to cardiomyocyte area. All analyses were completed by a blinded investigator, as described.[19]

LV flow cytometry

In a separate cohort of mice, LV tissue was digested and stained with fluorescent antibodies to quantify the number of total leukocytes (CD45+), T cells (CD3+/CD11b−) and myeloid cells (CD3−/CD11b+) by flow cytometry as in [23] and Supplemental Figure 1.

RT-qPCR

RNA was extracted from apical and basal LV regions and RT-qPCR was performed as described[19] using gene specific primers (Supplemental Table 2).

Statistical Analysis

Values are presented as mean ± SEM. One-way or two-way analysis of variance (ANOVA) was performed as indicated in each figure legend followed by Tukey post-hoc test using SigmaPlot 12.5 (Systat Software Inc) and Graph Pad Prism version 8. Grubb's test was used resulting in removal of one statistical outlier from the SMC-MR intact TAC group for gene expression. There were no significant violations of normality in the data obtained. Statistical significance was set at $P < 0.05$.

Results

SMC-MR deletion attenuates cardiac dysfunction induced by pressure overload

Prior to TAC, cardiac structure and function were determined by ultrasound and was not different between SMC-MR-KO mice and MR-intact littermates (Supplemental Table 1). Mice were then randomized to pressure overload via TAC or to sham surgery and the impact on cardiac function was quantified 4 weeks later by cardiac ultrasound and invasive hemodynamics. TAC induced a statistically significant reduction in LV EF and fractional shortening (FS) in MR-intact mice (Figure 1A-C). SMC-MR deletion ameliorated the reduction in EF and FS induced by TAC. Regardless of the presence of SMC-MR, there was a similar rise in proximal aortic pressure induced by TAC and no statistically significant difference in aortic stiffness as measured by pulse wave velocity (Table 1). TAC-induced mortality after 4 weeks was not statistically different between groups, supporting that the results are not biased by those that survived. The improvement in cardiac function by non-invasive imaging in SMC-MR-KO TAC mice is consistent with invasive measures of stroke volume and cardiac output which were also significantly increased in SMC-MR-KO compared to MR-intact mice exposed to TAC. Similarly, quantification of the maximal and minimal rate of rise in LV pressure (dP/dt max, dP/dt min) confirm TAC-induced cardiac

dysfunction that was statistically significantly attenuated by SMC-MR KO (Figs 1D-E). TAC induced an increase in LV systolic and diastolic stiffness as measured by the slope of the end systolic or diastolic pulse velocity relationship (ESPVR, EDPVR) and this TAC-induced cardiac stiffness was attenuated in SMC-MR-KO compared to MR-intact mice (Figs. 1F-G). Other parameters are summarized in Supplemental Table 3.

SMC-MR deletion prevents TAC-induced cardiac dilation and HF

Once the impact of TAC exceeds the ability of the heart to compensate for pressure overload, the heart begins to dilate, intra-cardiac pressure rises and pulmonary edema and exercise intolerance develop as the heart fails. Four weeks after TAC, MR-intact mice developed cardiac dilation manifest by an increase in left ventricular end systolic diameter (ESD) and end diastolic diameter (EDD, Figure 2A-B). SMC-MR-KO mice developed less systolic dilation compared to MR-intact TAC mice and no statistical change in diastolic chamber dimension compared to genotype matched sham mice. The TAC-induced rise in LV end diastolic pressure (EDP) was also reduced in SMC-MR-KO mice (Figure 2C). Importantly, SMC-MR-KO mice did not develop pulmonary edema, as measured by the difference between lung wet and dry weight (Fig 2D). The development of hemodynamically significant HF activates the renin-angiotensin-aldosterone (RAAS) system, as demonstrated by a rise in serum aldosterone in MR-intact mice exposed to TAC, which also did not occur in the SMC-MR-KO mice (Fig. 2E). Finally, as a measurement of the whole body cardiorespiratory function, endurance exercise capacity was assessed, and the decline in exercise capacity induced by TAC was attenuated in SMC-MR-KO mice (Fig. 2F).

SMC-MR contributes to pathological cardiac hypertrophy induced by TAC

We next quantified the effects of SMC-MR KO on cardiac hypertrophy (Figure 3). Total heart weight (Table 1) and LV weight normalized to tibia length were statistically significantly increased in response to TAC and this degree of hypertrophy was attenuated in SMC-MR-KO mice (Fig. 3A). A similar result was obtained for posterior wall thickness detected by echocardiography (Fig. 3B). Similarly, cardiomyocyte area was increased by TAC versus and this was attenuated in SMC-MR-KO mice (Fig. 3C). Cardiac expression of pathological hypertrophy genes was quantified by RT-qPCR in LV apical tissue. Atrial natriuretic peptide (*ANP*) and brain natriuretic peptide (*BNP*) expression were up-regulated in response to TAC and this was prevented in SMC-MR-KO TAC mice (Figs. 3D-E). Myosin heavy chain 6 (*Myh6*) gene expression was unchanged by TAC, but the fetal isoform, myosin heavy chain 7 (*Myh7*), was increased resulting in a significant increase in the *Myh7/Myh6* ratio in TAC versus Sham MR-intact mice. This isoform switch did not occur in SMC-MR-KO TAC mice (Fig. 3F).

SMC-MR deletion reduces TAC-induced cardiac fibrosis

Next, cardiac fibrosis was assessed by quantifying LV collagen deposition (Figure 4). Cardiac fibrosis was significantly increased by TAC. Both perivascular and interstitial fibrosis were attenuated in SMC-MR-KO compared to MR-intact TAC mice (Figs. 4A-B). Fibrotic gene expression was quantified by RT-qPCR in LV apical tissue (Figure 4C-H). In MR-intact mice, TAC induced a statistically significant increase in mRNA expression of

connective tissue growth factor (*CTGF*), collagen type 1 alpha (*Col1a*), collagen type 3 alpha (*Col3a*) mRNA, alpha smooth muscle actin (*alpha-SMA*) and transforming growth factor beta 1 (*TGFβ1*). The increase in fibrosis gene expression was prevented in SMC-MR-KO mice with SMC-MR-KO TAC mice having statistically less *CTGF, Col1a, Col3a, alpha-SMA, and TGFβ1* mRNA expression compared to MR-intact TAC mice. Matrix metalloproteinase-2 (*MMP2*) mRNA expression was not statistically different in response to TAC or MR deletion.

SMC-MR contributes to TAC-induced cardiac inflammation

The impact of SMC-MR deletion on cardiac inflammation was next examined (Figure 5). Cardiac leukocyte infiltration was quantified by flow cytometry and immunohistochemistry in a subset of mice. As there was no genotype difference in cardiac inflammation in sham operated mice thus, these groups were combined for analysis (Fig 5A-C). While there tended to be more CD45+ inflammatory cells in TAC compared to sham hearts, this was not statistically significant at 4 weeks post TAC (Fig. 5A, P=0.08). Among CD45+ leukocytes, there was a statistically significant increase in CD3−/CD11b+ myeloid cells (but not CD3+/CD11b− T cells) in the hearts of MR-intact TAC mice compared to sham but not in SMC-MR-KO mice exposed to pressure overload (Figs. 5B-C, Supplemental Figure 1). Immunohistochemistry similarly showed a non-statistically significant trend towards increased T cells in MR-intact mice exposed to TAC (Supplemental Figure 2). Expression of inflammatory cytokine genes including *RANTES* (regulated on activation normal T cell expressed and secreted), interleukin 1 beta (*IL1β*), and interleukin 6 (*IL6*) were up-regulated in LV tissue 4 weeks after TAC in MR-intact mice but not in SMC-MR-KO mice (Figs 5D-H). There was no statistically significant change in tumor necrosis factor alpha (*TNFα*) or monocyte chemoattractant protein-1 (*MCP-1*) expression 4 weeks after TAC. We recently implicated endothelial cell (EC)-MR in regulating cell adhesion molecules and selectins in the systemic vasculature. Thus, we examined gene expression of intercellular adhesion molecule 1 (*ICAM1*), vascular cell adhesion protein 1 (*VCAM1*) and the endothelial adhesion molecule, *E-selectin*. *ICAM1* and *VCAM1* mRNA were increased in MR-intact TAC mice compared to genotype-matched sham mice, but not in SMC-MR-KO TAC mice, with significantly lower expression in SMC-MR-KO compared to MR-intact mice exposed to TAC (Figs 5I-J). *E-selectin* expression was not significantly altered by TAC or SMC-MR deletion (Figure 5K).

SMC-MR deletion attenuates the pressure overload-induced decline in capillary density and coronary flow reserve

To further explore mechanisms by which SMC-MR might contribute to adverse cardiac remodeling and the resulting LV dysfunction, the impact of SMC-MR-KO on cardiac blood supply was examined. Cardiac blood supply can be augmented chronically by angiogenesis to increase capillary density or acutely by vasodilation of coronary resistance vessels. TAC induced a statistically significant increase in expression of two angiogenic genes, fibroblast growth factor (FGF2) and placental growth factor (PGF) with no change in the VEGF receptor, Flt1 (Figs 6A-C). This induction of angiogenic gene expression was not present in SMC-MR-KO mice. Capillary density, as measured by CD31 positive endothelial cell area normalized to cardiomyocyte area, was significantly decreased by TAC in both MR-intact

and SMC-MR-KO mice. This decrease in capillary density induced by pressure overload was attenuated in SMC-MR-KO mice (Figure 6D-E). Finally, we quantified CFR which measures the capacity to acutely dilate coronary vessels to meet demand. CFR was assessed by ultrasound four weeks after TAC by measuring coronary flow velocity before and after exposure to a hyperemic stimulus (2.5% isoflurane). As with capillary density, CFR was significantly decreased by TAC in both MR-intact and SMC-MR-KO mice however there was a statistically significant increase in CFR in SMC-MR-KO compared to MR-intact TAC mice (Figure 6F). Overall, SMC-MR deletion statistically improved cardiac capillary density and the capacity to augment coronary vessel blood flow in the setting of pressure overload-induced HF.

Discussion

In summary, these data demonstrate for the first time that SMC-MR contributes substantially to HF pathophysiology induced by pressure overload. In the severe TAC model, SMC-MR deletion protects mice from pathological cardiac hypertrophy, adverse cardiac remodeling and HF development. SMC-MR deletion prevented or statistically attenuated cardiomyocyte hypertrophy, cardiac inflammation, LV interstitial and perivascular fibrosis, cardiac dilation, systolic function decline and pulmonary edema. SMC-MR deletion preserved cardiac microvascular density and improved CFR in association with improved exercise capacity. Together, these data summarized in Table 2, provide a novel paradigm for how MR inhibition may improve outcomes in HF. Inhibiting SMC-MR may improve cardiac blood supply during hypertrophy, thereby attenuating pathological remodeling. The resulting decrease in lung edema and improved exercise capacity could contribute to the significant reduction in hospitalization and death in HF patients treated chronically with MR antagonists.[1]

As in clinical trials, MR antagonists are also protective in animal HF models. In the TAC model, treatment with spironolactone or eplerenone, MR antagonists used to treat HF patients, attenuated cardiac hypertrophy, LV dilation, systolic dysfunction, cardiac inflammation and fibrosis (Table 2).[11-13, 27] Cell-specific KO mice have been employed to explore potential mechanisms for the benefits of MR inhibition in HF induced by TAC (Table 2). As MR inhibition substantially limits adverse cardiac remodeling and fibrosis, the prevailing theory had been that the benefits are due to blockade of MR in cardiomyocytes or fibroblasts. However, fibroblast MR deletion had no impact on the pathophysiology of TAC-induced HF. In mice with cardiomyocyte MR deletion, LV systolic function was relatively preserved and cardiac dilatation was attenuated. However, there was no significant impact of cardiomyocyte MR KO on the degree of cardiac hypertrophy, inflammation, fibrosis, or cardiomyocyte apoptosis supporting the concept that MR in other cells might contribute to HF pathophysiology.[14] Studies exploring EC-MR in TAC-induced HF similarly demonstrated modest protection from LV systolic dysfunction with no statistically significant impact of EC-MR deletion on cardiac hypertrophy, inflammation, angiogenesis or fibrosis (although with a less severe 25 gauge TAC).[15] Recent studies have explored the role of leukocyte MR in pressure overload-induced HF using the abdominal (rather than thoracic) aortic constriction (AAC) model which induces more substantial alterations in aortic, in additional to cardiac, pathology.[28, 29] Myeloid MR deletion attenuated the decline

in cardiac hypertrophy, fibrosis and inflammation although cardiac function and blood supply were not measured. T cell MR deletion decreased early cardiac inflammation (1 week post AAC) and this was associated with decreased cardiac hypertrophy, fibrosis, and systolic dysfunction at 6 weeks.[28, 29] Thus, leukocyte MR likely also plays an important role in HF, but the different model and timing used in those leukocyte MR studies precludes direct comparison with other study. To our knowledge, the present study is the first to explore the role of SMC-MR in any animal model of pressure overload-induced HF. The results reveal that SMC-MR deletion protects from all aspects of TAC-induced pathology including cardiac hypertrophy, dilation, inflammation, fibrosis, and systolic dysfunction, with improvement in important clinical endpoints including lung edema and exercise capacity, all in the setting of increased capillary density and improved coronary flow reserve.

These new data, combined with published studies, support several molecular mechanisms by which SMC-MR may contribute to adverse cardiac remodeling. Early in the development of pressure overload-induced HF, inflammatory cells infiltrate the heart and contribute to cardiac fibrosis.[30] MR is a hormone-activated transcription factor that regulates gene expression. TAC-induced cardiac leukocyte recruitment requires expression of the adhesion molecule ICAM1 but surprisingly, this was found to be independent of EC-MR, a known regulator of ICAM1 transcription.[15, 31, 32] Once recruited to the heart, leukocytes promote expression of pro-inflammatory mediators that contribute to the development of adverse cardiac remodeling and fibrosis. Here we show that TAC-induced upregulation of ICAM1 (and VCAM1) and inflammatory mediators including RANTES, IL1β, and IL6 are either prevented or statistically attenuated in SMC-MR-KO mice. As expected, by four weeks after TAC, there is only a modest increase in leukocyte infiltration which was not statistically significantly attenuated in SMC-MR-KO mice, however, earlier TAC time points would be needed to clarify this. Previous studies demonstrated that human SMC-MR transcriptionally regulates the release of leukocyte chemotactic factors including placental growth factor (PGF).[33] Here we show that PGF mRNA expression in cardiac tissue is increased in response to TAC in MR-intact mice and this is prevented in mice lacking SMC-MR. Thus, one potential mechanism by which SMC-MR contributes to adverse vascular remodeling may be by regulating expression of inflammatory and adhesion molecules that contribute to cardiac inflammation.

Substantial literature supports a role for SMC-MR in promoting vascular fibrosis in mouse models of hypertension, vascular injury, and aging (reviewed in [34, 35]). MR activation in human SMC and mouse vessels regulates expression of a gene program that includes type 1 and 3 collagen, CTGF, MMP2 and other pro-fibrotic genes.[18, 19, 36] This study demonstrates TAC-induced upregulation of fibrosis gene mRNA expression in the heart is significantly attenuated in SMC-MR-KO mice, in association with less perivascular and interstitial fibrosis and abrogation of cardiac dilation and dysfunction. Thus, SMC-MR may also contribute to adverse cardiac remodeling and HF by coordination transcription of a pro-fibrotic gene program induced by pressure overload.

Finally, our study supports that SMC-MR may contribute to impaired blood supply to the heart in response to pressure overload. Blood supply to the heart can be modulated acutely to response to demand by vasodilation or constriction of coronary resistance vessels, a process

which is mediated by SMCs and can be quantified by assessing coronary flow reserve (CFR). Chronically, blood supply may be enhanced by increased capillary density via angiogenesis which is driven by hypoxia-inducible angiogenic factors. A mismatch between cardiac hypertrophy and microvascular density has been previously implicated in pathological cardiac remodeling and the associated tissue hypoxia may lead to cardiac dysfunction. This phenomenon may be observed by the increase in angiogenic gene expression observed in MR-intact TAC mice.[37, 38] Our data reveals that SMC-MR deletion is associated with decreased cardiac hypertrophy and protection against the decline in capillary density and CFR. The resulting improvement in blood supply relative to demand may contribute to the improvement in cardiac function and HF outcomes in SMC-MR-KO mice. In addition to the potential impact on angiogenesis, SMC-MR has been shown to contribute to vasoconstriction by regulating L-type calcium channels and angiotensin II receptor expression and contributing to oxidative stress.[17, 20, 39] In a coronary ligation model, SMC-MR deletion improved coronary vasodilation.[40] Furthermore, in a clinical trial of patients with diabetes, MR inhibition improved CFR.[41] Here we demonstrate for the first time that CFR, the capacity to dilate the coronary vessels to meet demand, is impaired by TAC and that this is improved in SMC-MR-KO mice (Table 2). This may be due to improvements in coronary vasodilatory function as well as changes in vascular structure mediated by SMC-MR.

Several limitations to this study must be acknowledged. First, the data presented were generated with male mice. All published murine TAC studies investigating MR deletion or inhibition only used males (Table 2), thus our study was designed to directly compare to this published work. This limitation precludes application of these results to females. A recent systematic review of over 500 TAC manuscripts revealed that only 4% used female mice with 67% using only males, 20% not reporting the sex, and 9% mixing males and females.[42] One potential reason is that due to the smaller size of female mice, TAC with the same gauge needle does not induce the same degree of pressure overload making direct comparison between the sexes extremely challenging. Thus, future detailed studies are needed to generate comparable TAC gradients in both sexes before examining the role of SMC-MR in HF in females. Second, although no murine model recapitulates all aspects of the human HF, we focused on the severe 27 gauge TAC model because it reproduces many of the pathophysiological endpoints observed in human HF and it has been used most extensively to study MR tissue-specific effects during HF (Table 2). Future studies are needed to determine if SMC-MR plays a similar role in other models of HF. As an example, while MR deletion from cardiomyocytes did not significantly impact LV remodeling in the TAC model[14], in a chronic coronary ligation model, cardiomyocyte MR deletion improved capillary density and decreased cardiac hypertrophy and fibrosis.[43]

Despite these limitations, this study has clinical implications as it provides a novel mechanism that may contribute to the benefits of MR antagonism in HF patients. In patients with HFrEF, MR inhibition improves cardiac remodeling, prevents hospitalization and decreases mortality.[1] This study supports that some of those benefits might be mediated by SMC-MR inhibition resulting in decreased cardiac inflammation and fibrosis while improving blood flow and decreasing hypertrophy; together this may prevent the adverse cardiac remodeling that leads to progressive HF and death. Other studies exploring cell-

specific roles of MR did not measure pulmonary edema or exercise capacity, thus it is unclear if MR in other cell types, some of which have benefits on cardiac structure or function, might also improve HF symptom outcomes. These are important parameters that are relevant to HF hospitalization and mortality in humans. Another important controversy is whether MR inhibition is beneficial in HFpEF. In the TOPCAT trial of spironolactone in HFpEF patients, MR inhibition did not significantly decrease mortality.[44] However, HF hospitalization was decreased and subgroups of HFpEF patients may have benefited from MR inhibition.[45, 46] In the current study, SMC-MR deletion attenuated cardiac hypertrophy, stiffness and fibrosis after TAC. These may be potential mechanisms for benefits of MR antagonists on diastolic function. If this is unique to the pressure overload model, this might suggest specific etiologies of HFpEF (i.e. HFpEF induced by hypertension or valve disease) may benefit more from MR inhibition, a hypothesis which remains to be tested in clinical trials.

Overall, this study demonstrates that SMC-MR contributes substantially to the development of HF in the TAC model. SMC-MR deletion attenuates cardiac inflammation, prevents profibrotic gene expression limiting cardiac fibrosis and adverse remodeling, and preserves capillary density and CFR providing enhanced blood supply in the face of cardiac hypertrophy. Together, these mechanisms support a substantial role for SMC-MR in the benefits of MR inhibition in attenuating pulmonary edema and improving cardiac function and exercise capacity in pressure-overload induced HF.

Supplementary Material

Refer to Web version on PubMed Central for supplementary material.

Acknowledgements:

We thank Nathan Li at the Tufts Animal Histology Core for his technical support.

Sources of Funding:

This work was supported by grants from the National Institutes of Health: T32HL007609 (to LAB), F30 HL152505 (to JJM), F30HL137255 (to MEM), HL123658 (to PA), HL095590 and HL119290 (to IZJ), the American Heart Association: 19POST34430075/2019 (to FJC-S) and EIA18290005 (to IZJ), and the National Research Foundation of Korea (NRF) grant funded by the Korea government (MSIT) (No. 2020R1F1A1073394) (to SKK).

Non-standard Abbreviations and Acronyms

AAC	Abdominal aortic constriction
ANP	atrial natriuretic peptide
BNP	Brain natriuretic peptide
CFR	Coronary flow reserve
EC	Endothelial cells
EDD	End diastolic diameter

EDPVR	end diastolic pulse velocity relationship
ESD	End systolic diameter
ESPVR	end systolic pulse velocity relationship
EF	Ejection fraction
FS	Fractional shortening
HF	Heart failure
HFpEF	Heart failure with preserved ejection fraction
HFrEF	Heart failure with reduced ejection fraction
LV	Left ventricle
MR	Mineralocorticoid receptor
PV	pressure-volume
SMC	Smooth muscle cells
SMC-MR-KO	Smooth muscle mineralocorticoid receptor knockout mouse
TAC	Transverse aortic constriction

References

1. Pitt B, Zannad F, Remme WJ, Cody R, Castaigne A, Perez A, Palensky J,Wittes J. The effect of spironolactone on morbidity and mortality in patients with severe heart failure. Randomized Aldactone Evaluation Study Investigators. N Engl J Med. 1999;341:709–717. [PubMed: 10471456]
2. Pitt B, Remme W, Zannad F, Neaton J, Martinez F, Roniker B, Bittman R, Hurley S, Kleiman J, Gatlin M, Eplerenone Post-Acute Myocardial Infarction Heart Failure E,Survival Study I. Eplerenone, a selective aldosterone blocker, in patients with left ventricular dysfunction after myocardial infarction. N Engl J Med. 2003;348:1309–1321. [PubMed: 12668699]
3. Zannad F, McMurray JJ, Krum H, van Veldhuisen DJ, Swedberg K, Shi H, Vincent J, Pocock SJ, Pitt B,Group E-HS. Eplerenone in patients with systolic heart failure and mild symptoms. N Engl J Med. 2011;364:11–21. [PubMed: 21073363]
4. Ezekowitz JA,McAlister FA. Aldosterone blockade and left ventricular dysfunction: a systematic review of randomized clinical trials. Eur Heart J. 2009;30:469–477. [PubMed: 19066207]
5. Chen Y, Wang H, Lu Y, Huang X, Liao Y,Bin J. Effects of mineralocorticoid receptor antagonists in patients with preserved ejection fraction: a meta-analysis of randomized clinical trials. BMC Med. 2015;13:10. [PubMed: 25598008]
6. Pitt B Do diuretics and aldosterone receptor antagonists improve ventricular remodeling? J Card Fail. 2002;8:S491–493. [PubMed: 12555163]
7. Li X, Qi Y, Li Y, Zhang S, Guo S, Chu S, Gao P, Zhu D, Wu Z, Lu L, Shen W, Jia N,Niu W. Impact of mineralocorticoid receptor antagonists on changes in cardiac structure and function of left ventricular dysfunction: a meta-analysis of randomized controlled trials. Circ Heart Fail. 2013;6:156–165. [PubMed: 23400891]
8. Richards DA, Aronovitz MJ, Calamaras TD, Tam K, Martin GL, Liu P, Bowditch HK, Zhang P, Huggins GS,Blanton RM. Distinct Phenotypes Induced by Three Degrees of Transverse Aortic Constriction in Mice. Sci Rep. 2019;9:5844. [PubMed: 30971724]

9. Pitoulis FG,Terracciano CM. Heart Plasticity in Response to Pressure- and Volume-Overload: A Review of Findings in Compensated and Decompensated Phenotypes. Front Physiol. 2020;11:92. [PubMed: 32116796]
10. Ding Y, Wang Y, Jia Q, Wang X, Lu Y, Zhang A, Lv S,Zhang J. Morphological and Functional Characteristics of Animal Models of Myocardial Fibrosis Induced by Pressure Overload. Int J Hypertens. 2020;2020:3014693. [PubMed: 32099670]
11. Franco V, Chen YF, Feng JA, Li P, Wang D, Hasan E, Oparil S,Perry GJ. Eplerenone prevents adverse cardiac remodelling induced by pressure overload in atrial natriuretic peptide-null mice. Clin Exp Pharmacol Physiol. 2006;33:773–779. [PubMed: 16922805]
12. Ayuzawa N, Nagase M, Ueda K, Nishimoto M, Kawarazaki W, Marumo T, Aiba A, Sakurai T, Shindo T,Fujita T. Rac1-Mediated Activation of Mineralocorticoid Receptor in Pressure Overload-Induced Cardiac Injury. Hypertension. 2016;67:99–106. [PubMed: 26527051]
13. Kuster GM, Kotlyar E, Rude MK, Siwik DA, Liao R, Colucci WS,Sam F. Mineralocorticoid receptor inhibition ameliorates the transition to myocardial failure and decreases oxidative stress and inflammation in mice with chronic pressure overload. Circulation. 2005;111:420–427. [PubMed: 15687129]
14. Lother A, Berger S, Gilsbach R, Rosner S, Ecke A, Barreto F, Bauersachs J, Schutz G,Hein L. Ablation of mineralocorticoid receptors in myocytes but not in fibroblasts preserves cardiac function. Hypertension. 2011;57:746–754. [PubMed: 21321305]
15. Salvador AM, Moss ME, Aronovitz M, Mueller KB, Blanton RM, Jaffe IZ,Alcaide P. Endothelial mineralocorticoid receptor contributes to systolic dysfunction induced by pressure overload without modulating cardiac hypertrophy or inflammation. Physiol Rep. 2017;5.
16. Parker BM, Wertz SL, Pollard CM, Desimine VL, Maning J, McCrink KA,Lymperopoulos A. Novel Insights into the Crosstalk between Mineralocorticoid Receptor and G Protein-Coupled Receptors in Heart Adverse Remodeling and Disease. Int J Mol Sci. 2018;19.
17. DuPont JJ, McCurley A, Davel AP, McCarthy J, Bender SB, Hong K, Yang Y, Yoo JK, Aronovitz M, Baur WE, Christou DD, Hill MA,Jaffe IZ. Vascular mineralocorticoid receptor regulates microRNA-155 to promote vasoconstriction and rising blood pressure with aging. JCI Insight. 2016;1:e88942. [PubMed: 27683672]
18. Jaffe IZ,Mendelsohn ME. Angiotensin II and aldosterone regulate gene transcription via functional mineralocortocoid receptors in human coronary artery smooth muscle cells. Circ Res. 2005;96:643–650. [PubMed: 15718497]
19. Kim SK, McCurley AT, DuPont JJ, Aronovitz M, Moss ME, Stillman IE, Karumanchi SA, Christou DD,Jaffe IZ. Smooth Muscle Cell-Mineralocorticoid Receptor as a Mediator of Cardiovascular Stiffness With Aging. Hypertension. 2018;71:609–621. [PubMed: 29463624]
20. McCurley A, Pires PW, Bender SB, Aronovitz M, Zhao MJ, Metzger D, Chambon P, Hill MA, Dorrance AM, Mendelsohn ME,Jaffe IZ. Direct regulation of blood pressure by smooth muscle cell mineralocorticoid receptors. Nat Med. 2012;18:1429–1433. [PubMed: 22922412]
21. Chang WT, Fisch S, Chen M, Qiu Y, Cheng S,Liao R. Ultrasound based assessment of coronary artery flow and coronary flow reserve using the pressure overload model in mice. J Vis Exp. 2015:e52598. [PubMed: 25938185]
22. Cross TJ, Kim CH, Johnson BD,Lalande S. The interactions between respiratory and cardiovascular systems in systolic heart failure. J Appl Physiol (1985). 2020;128:214–224. [PubMed: 31774354]
23. Ngwenyama N, Salvador AM, Velazquez F, Nevers T, Levy A, Aronovitz M, Luster AD, Huggins GS,Alcaide P. CXCR3 regulates CD4+ T cell cardiotropism in pressure overload-induced cardiac dysfunction. JCI Insight. 2019;4.
24. Yang F, Dong A, Mueller P, Caicedo J, Sutton AM, Odetunde J, Barrick CJ, Klyachkin YM, Abdel-Latif A,Smyth SS. Coronary artery remodeling in a model of left ventricular pressure overload is influenced by platelets and inflammatory cells. PLoS One. 2012;7:e40196. [PubMed: 22916095]
25. Muller P, Kazakov A, Semenov A, Bohm M,Laufs U. Pressure-induced cardiac overload induces upregulation of endothelial and myocardial progenitor cells. Cardiovasc Res. 2008;77:151–159. [PubMed: 18006457]

26. Qu J, Volpicelli FM, Garcia LI, Sandeep N, Zhang J, Marquez-Rosado L, Lampe PD,Fishman GI. Gap junction remodeling and spironolactone-dependent reverse remodeling in the hypertrophied heart. Circ Res. 2009;104:365–371. [PubMed: 19096029]
27. Grune J, Benz V, Brix S, Salatzki J, Blumrich A, Hoft B, Klopfleisch R, Foryst-Ludwig A, Kolkhof P,Kintscher U. Steroidal and Nonsteroidal Mineralocorticoid Receptor Antagonists Cause Differential Cardiac Gene Expression in Pressure Overload-induced Cardiac Hypertrophy. J Cardiovasc Pharmacol. 2016;67:402–411. [PubMed: 26859196]
28. Li C, Sun XN, Zeng MR, Zheng XJ, Zhang YY, Wan Q, Zhang WC, Shi C, Du LJ, Ai TJ, Liu Y, Liu Y, Du LL, Yi Y, Yu Y,Duan SZ. Mineralocorticoid Receptor Deficiency in T Cells Attenuates Pressure Overload-Induced Cardiac Hypertrophy and Dysfunction Through Modulating T-Cell Activation. Hypertension. 2017;70:137–147. [PubMed: 28559389]
29. Li C, Zhang YY, Frieler RA, Zheng XJ, Zhang WC, Sun XN, Yang QZ, Ma SM, Huang B, Berger S, Wang W, Wu Y, Yu Y, Duan SZ,Mortensen RM. Myeloid mineralocorticoid receptor deficiency inhibits aortic constriction-induced cardiac hypertrophy in mice. PLoS One. 2014;9:e110950. [PubMed: 25354087]
30. Nevers T, Salvador AM, Grodecki-Pena A, Knapp A, Velazquez F, Aronovitz M, Kapur NK, Karas RH, Blanton RM,Alcaide P. Left Ventricular T-Cell Recruitment Contributes to the Pathogenesis of Heart Failure. Circ Heart Fail. 2015;8:776–787. [PubMed: 26022677]
31. Caprio M, Newfell BG, la Sala A, Baur W, Fabbri A, Rosano G, Mendelsohn ME,Jaffe IZ. Functional mineralocorticoid receptors in human vascular endothelial cells regulate intercellular adhesion molecule-1 expression and promote leukocyte adhesion. Circ Res. 2008;102:1359–1367. [PubMed: 18467630]
32. Salvador AM, Nevers T, Velazquez F, Aronovitz M, Wang B, Abadia Molina A, Jaffe IZ, Karas RH, Blanton RM,Alcaide P. Intercellular Adhesion Molecule 1 Regulates Left Ventricular Leukocyte Infiltration, Cardiac Remodeling, and Function in Pressure Overload-Induced Heart Failure. J Am Heart Assoc. 2016;5:e003126. [PubMed: 27068635]
33. McGraw AP, Bagley J, Chen WS, Galayda C, Nickerson H, Armani A, Caprio M, Carmeliet P,Jaffe IZ. Aldosterone increases early atherosclerosis and promotes plaque inflammation through a placental growth factor-dependent mechanism. J Am Heart Assoc. 2013;2:e000018. [PubMed: 23525413]
34. Biwer LA, Wallingford MC,Jaffe IZ. Vascular Mineralocorticoid Receptor: Evolutionary Mediator of Wound Healing Turned Harmful by Our Modern Lifestyle. Am J Hypertens. 2019;32:123–134. [PubMed: 30380007]
35. Koenig JB,Jaffe IZ. Direct role for smooth muscle cell mineralocorticoid receptors in vascular remodeling: novel mechanisms and clinical implications. Curr Hypertens Rep. 2014;16:427. [PubMed: 24633842]
36. Galmiche G, Pizard A, Gueret A, El Moghrabi S, Ouvrard-Pascaud A, Berger S, Challande P, Jaffe IZ, Labat C, Lacolley P,Jaisser F. Smooth muscle cell mineralocorticoid receptors are mandatory for aldosterone-salt to induce vascular stiffness. Hypertension. 2014;63:520–526. [PubMed: 24296280]
37. Hoenig MR, Bianchi C, Rosenzweig A,Sellke FW. The cardiac microvasculature in hypertension, cardiac hypertrophy and diastolic heart failure. Curr Vasc Pharmacol. 2008;6:292–300. [PubMed: 18855717]
38. Mohammed SF, Hussain S, Mirzoyev SA, Edwards WD, Maleszewski JJ,Redfield MM. Coronary microvascular rarefaction and myocardial fibrosis in heart failure with preserved ejection fraction. Circulation. 2015;131:550–559. [PubMed: 25552356]
39. Amador CA, Bertocchio JP, Andre-Gregoire G, Placier S, Duong Van Huyen JP, El Moghrabi S, Berger S, Warnock DG, Chatziantoniou C, Jaffe IZ, Rieu P,Jaisser F. Deletion of mineralocorticoid receptors in smooth muscle cells blunts renal vascular resistance following acute cyclosporine administration. Kidney Int. 2016;89:354–362. [PubMed: 26422501]
40. Gueret A, Harouki N, Favre J, Galmiche G, Nicol L, Henry JP, Besnier M, Thuillez C, Richard V, Kolkhof P, Mulder P, Jaisser F,Ouvrard-Pascaud A. Vascular Smooth Muscle Mineralocorticoid Receptor Contributes to Coronary and Left Ventricular Dysfunction After Myocardial Infarction. Hypertension. 2016;67:717–723. [PubMed: 26902493]

41. Garg R, Rao AD, Baimas-George M, Hurwitz S, Foster C, Shah RV, Jerosch-Herold M, Kwong RY, Di Carli MF,Adler GK. Mineralocorticoid receptor blockade improves coronary microvascular function in individuals with type 2 diabetes. Diabetes. 2015;64:236–242. [PubMed: 25125488]

42. Bosch L, de Haan JJ, Bastemeijer M, van der Burg J, van der Worp E, Wesseling M, Viola M, Odille C, El Azzouzi H, Pasterkamp G, Sluijter JPG, Wever KE,de Jager SCA. The transverse aortic constriction heart failure animal model: a systematic review and meta-analysis. Heart Fail Rev. 2020.

43. Fraccarollo D, Berger S, Galuppo P, Kneitz S, Hein L, Schutz G, Frantz S, Ertl G,Bauersachs J. Deletion of cardiomyocyte mineralocorticoid receptor ameliorates adverse remodeling after myocardial infarction. Circulation. 2011;123:400–408. [PubMed: 21242479]

44. Pitt B, Pfeffer MA, Assmann SF, Boineau R, Anand IS, Claggett B, Clausell N, Desai AS, Diaz R, Fleg JL, Gordeev I, Harty B, Heitner JF, Kenwood CT, Lewis EF, O'Meara E, Probstfield JL, Shaburishvili T, Shah SJ, Solomon SD, Sweitzer NK, Yang S, McKinlay SM, Investigators T. Spironolactone for heart failure with preserved ejection fraction. N Engl J Med. 2014;370:1383–1392. [PubMed: 24716680]

45. Pfeffer MA, Claggett B, Assmann SF, Boineau R, Anand IS, Clausell N, Desai AS, Diaz R, Fleg JL, Gordeev I, Heitner JF, Lewis EF, O'Meara E, Rouleau JL, Probstfield JL, Shaburishvili T, Shah SJ, Solomon SD, Sweitzer NK, McKinlay SM,Pitt B. Regional variation in patients and outcomes in the Treatment of Preserved Cardiac Function Heart Failure With an Aldosterone Antagonist (TOPCAT) trial. Circulation. 2015;131:34–42. [PubMed: 25406305]

46. Lewis EF, Kim HY, Claggett B, Spertus J, Heitner JF, Assmann SF, Kenwood CT, Solomon SD, Desai AS, Fang JC, McKinlay SA, Pitt BA, Pfeffer MA, Investigators T. Impact of Spironolactone on Longitudinal Changes in Health-Related Quality of Life in the Treatment of Preserved Cardiac Function Heart Failure With an Aldosterone Antagonist Trial. Circ Heart Fail. 2016;9:e001937. [PubMed: 26962133]

What is new:

This study demonstrates for the first time that the mineralocorticoid receptor in smooth muscle cells contributes to heart failure induced by pressure overload.

Deletion of the mineralocorticoid receptor specifically from smooth muscle prevented cardiac hypertrophy, inflammation and fibrosis and improved systolic function with decreased lung edema and improved exercise capacity in a male mouse model of pressure overload-induced heart failure.

This may be due to preservation of cardiac capillary density and coronary blood flow during hypertrophy to prevent pathological cardiac remodeling.

What are the clinical implications:

Mineralocorticoid receptor antagonists improve outcomes in heart failure patients and this study supports that the benefits may be due in large part to effects of inhibiting the receptor in smooth muscle.

In patients with hypertension and valve disorders which induce pressure overload, MR inhibition in smooth muscle may prevent heart failure progression by improving cardiac blood flow and preventing adverse cardiac remodeling.

More broadly, the data support that the vasculature of the heart, and specifically the smooth muscle, may be a novel cellular target for heart failure therapies.

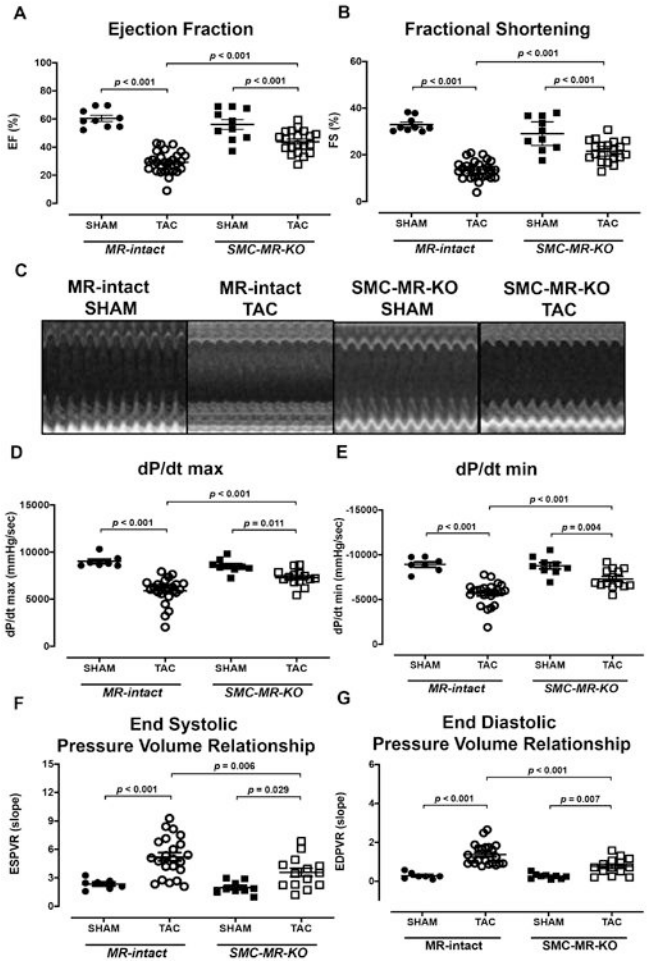

Figure 1: Deletion of mineralocorticoid receptor in smooth muscle cell (SMC-MR-KO) attenuates cardiac dysfunction induced by pressure overload

(A) LV ejection fraction (EF) and **(B)** fractional shortening (FS) measured by echocardiography. **(C)** Representative images of M-mode echocardiography. LV function indices assessed by invasive LV pressure-volume loop analysis to quantify **(D)** maximal rate of rise in LV pressure (dP/dt max), **(E)** minimal rate of rise in LV pressure (dP/dt min), **(F)** end-systolic pressure-volume relationship (ESPVR), a measure of systolic cardiac stiffness and **(G)** end-diastolic pressure-volume relationship (EDPVR), a measure of diastolic cardiac stiffness. A, B: MR-intact Sham n=9, MR-intact TAC n=27, SMC-MR-KO Sham n=10, SMC-MR-KO TAC n=17. D-G: MR-intact Sham n=7, MR-intact TAC n=23, SMC-MR-KO Sham n=9, SMC-MR-KO TAC n=14. Two-way ANOVA with Tukey post-hoc test.

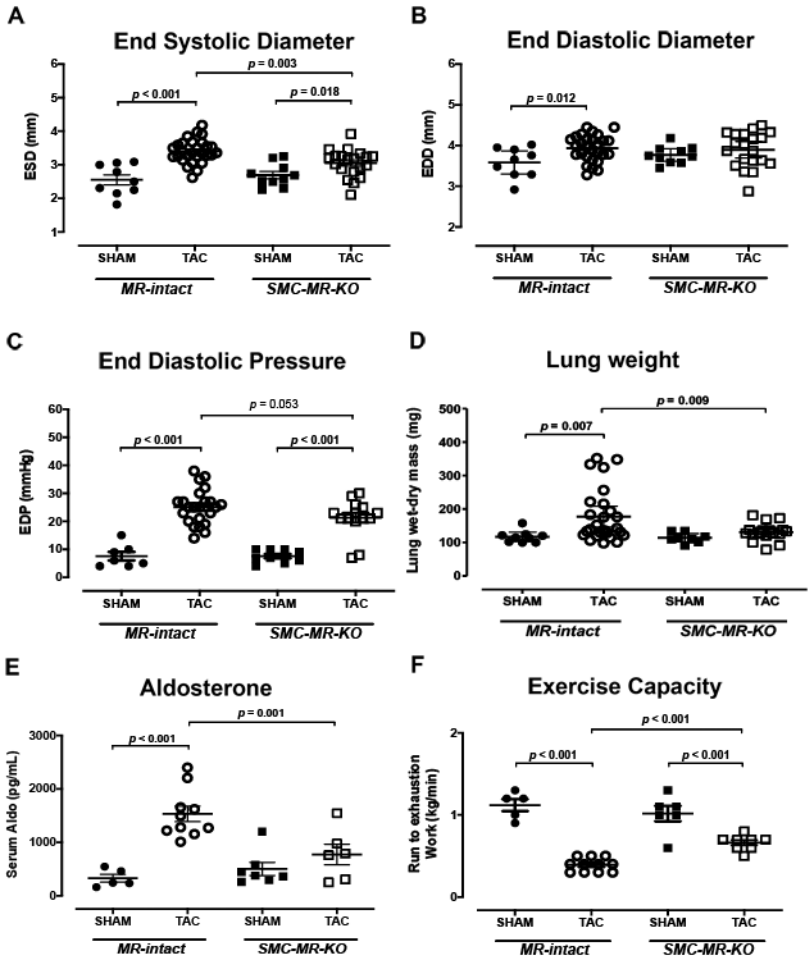

Figure 2: Deletion of mineralocorticoid receptor in smooth muscle cell (SMC-MR-KO) ameliorates pressure overload-induced cardiac dilation and heart failure.

(A) End-systolic diameter (ESD) and **(B)** end-diastolic diameter (EDD) of the left ventricle (LV) were measured by echocardiography; **(C)** LV end-diastolic pressure (EDP) as assessed by invasive left ventricular pressure-volume loop analysis; **(D)** Pulmonary edema as measured by lung wet mass minus dried mass; **(E)** Circulating aldosterone levels measured in serum; **(F)** Whole body endurance exercise capacity determined by measuring run to exhaustion time normalized to body mass and vertical distance on the rodent treadmill. A-D: MR-intact Sham n=9, MR-intact TAC n=27, SMC-MR-KO Sham n=10, SMC-MR-KO TAC n=17. E: MR-intact Sham n=5, MR-intact TAC n=10, SMC-MR-KO Sham n=7, SMC-MR-KO TAC n=6. F: MR-intact Sham n=5, MR-intact TAC n=11, SMC-MR-KO Sham n=6, SMC-MR-KO TAC n=8. Two-way ANOVA with Tukey post-hoc test.

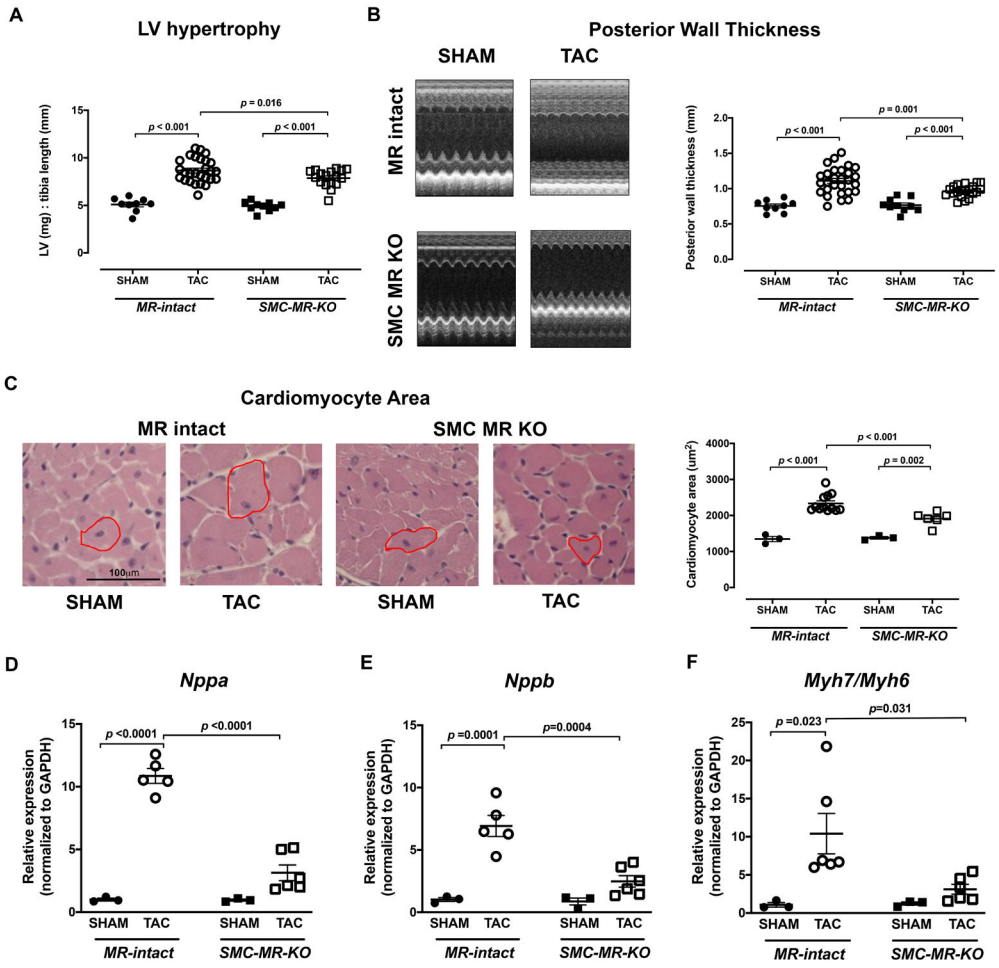

Figure 3: Mineralocorticoid receptor in smooth muscle cell (SMC-MR) contributes to pathological cardiac hypertrophy induced by pressure overload.

(A) LV hypertrophy measured by LV weight to tibia length ratio; **(B)** Left: Representative echocardiographic images used to quantify posterior wall thickness (PWT, right). **(C)** Left: Representative LV sections stained with H&E for assessment of cardiomyocyte area (red outline shows an example of a representative cardiomyocyte that was quantified) and quantification of cardiomyocyte area (right). Scale bar=100 μm. Results of quantitative RT-PCR for **(D)** atrial natriuretic peptide (Nppa), **(E)** brain natriuretic peptide (Nppb) and **(F)** the ratio of myosin heavy chain-β (Myh7) to myosin heavy chain-α (Myh6) in LV tissue. A, B: MR-intact Sham n=9, MR-intact TAC n=27, SMC-MR-KO Sham n=10, SMC-MR-KO TAC n=17. C: MR-intact Sham n=3, MR-intact TAC n=12, SMC-MR-KO Sham n=3, SMC-MR-KO TAC n=6. D-F: MR-intact Sham n=3, MR-intact TAC n=5, SMC-MR-KO Sham n=3, SMC-MR-KO TAC n=6. Two-way ANOVA with Tukey post-hoc test.

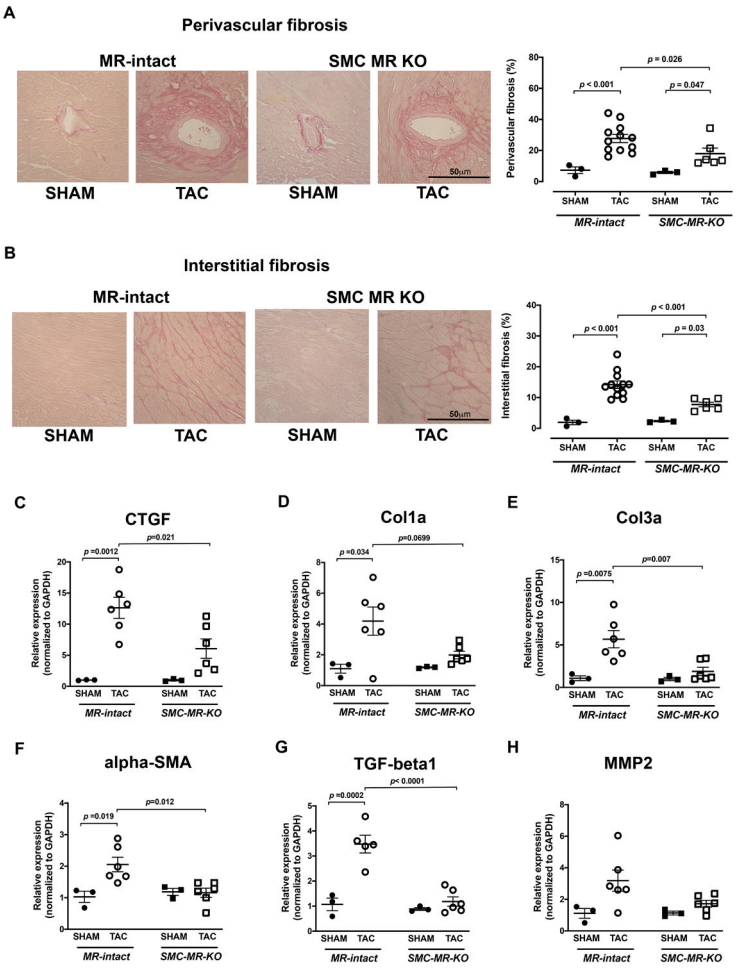

Figure 4: Deletion of mineralocorticoid receptor in smooth muscle cell (SMC-MR-KO) reduces pressure overload-induced cardiac fibrosis.

Representative LV sections stained with picrosirius red for assessment of perivascular (**A**) or interstitial (**B**) collagen deposition. Scale bar=50 μm. Results of quantitative RT-PCR with primers specific for: **(C)** connective tissue growth factor (CTGF); **(D)** collagen type 1 alpha (Col1α); **(E)** collagen type 3 alpha (Col3α); **(F)** alpha smooth muscle actin (alpha-SMA); **(G)** matrix metalloproteinase-2 (MMP2); and **(H)** transforming growth factor beta 1 (TGFβ1). A, B: MR-intact Sham n=3, MR-intact TAC n=12, SMC-MR-KO Sham n=3, SMC-MR-KO TAC n=6. C-H: MR-intact Sham n=3, MR-intact TAC n=6, SMC-MR-KO Sham n=3, SMC-MR-KO TAC n=6. Two-way ANOVA with Tukey post-hoc test.

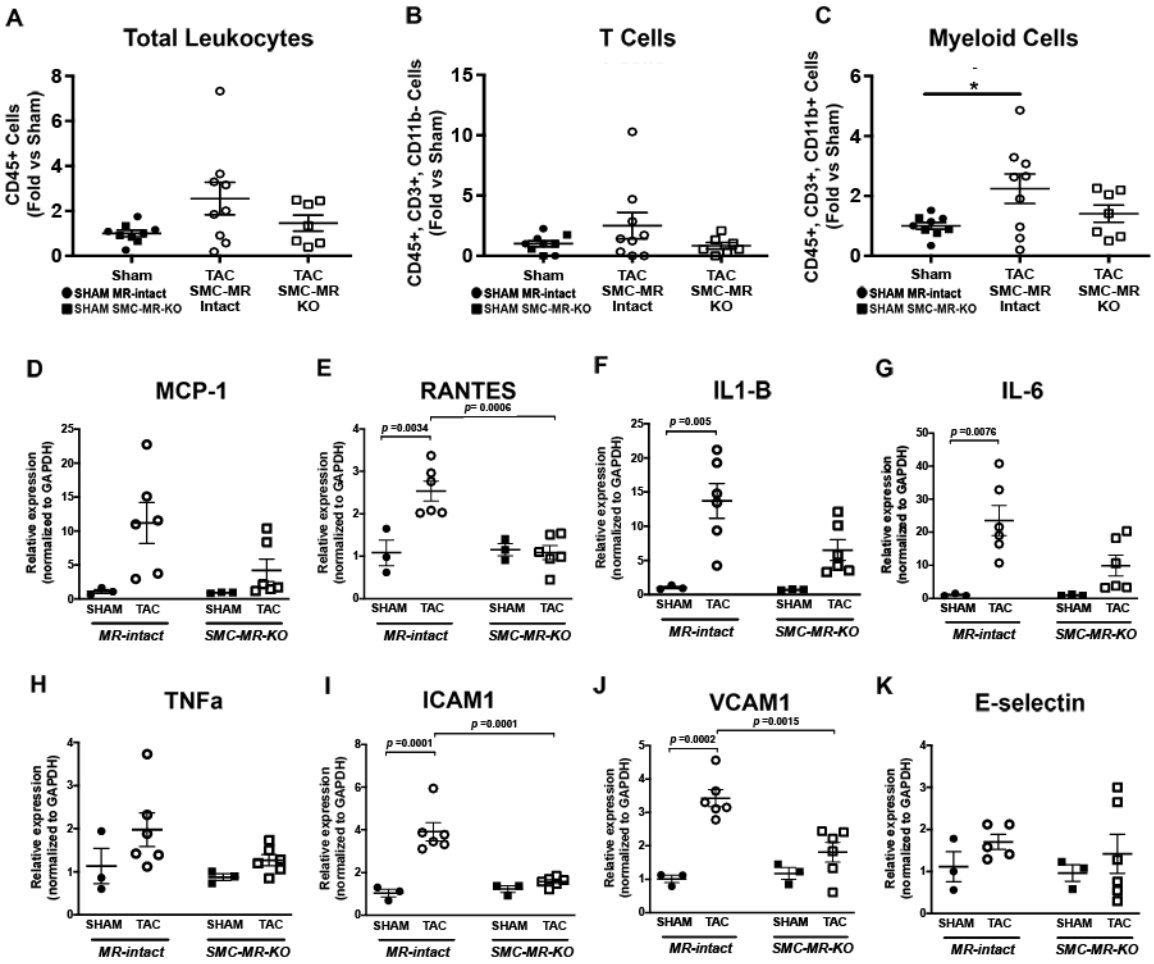

Figure 5: Deletion of mineralocorticoid receptor in smooth muscle cells (SMC-MR-KO) reduces pressure overload-induced cardiac inflammation.

Leukocytes were quantified from LV tissue 4 weeks after TAC by flow cytometry. **(A)** Total leukocytes (CD45+), **(B)** T cells (CD45+/CD11b−/CD3+) and **(C)** myeloid cells (CD45+/CD3−/CD11b+) were compared between Shams, MR-intact TAC or SMC-MR-KO TAC mice. Results of quantitative RT-PCR for inflammatory gene expression in the LV: **(D)** monocyte chemoattractant protein-1 (MCP-1), **(E)** regulated on activation, normal T cell expressed and secreted (RANTES), **(F)** interleukin 1 beta (IL1-B), **(G)** interleukin 6 (IL-6), and **(H)** tumor necrosis factor alpha (TNFα). Results of quantitative RT-PCR for adhesion molecules **(I)** intercellular adhesion molecule 1 (ICAM1), **(J)** vascular cell adhesion protein 1 (VCAM1), and **(K)** endothelial-leukocyte adhesion molecule (E-selectin). A-C: Sham n=9: (MR-intact Sham n=5, SMC-MR-KO Sham n=4), MR-intact TAC n=8, SMC-MR-KO TAC n=6. D-K: MR-intact Sham n=3, MR-intact TAC n=6, SMC-MR-KO Sham n=3, SMC-MR-KO TAC n=6. A-C: One-way ANOVA with Tukey post-hoc test. D-K: Two-way ANOVA with Tukey post-hoc test.

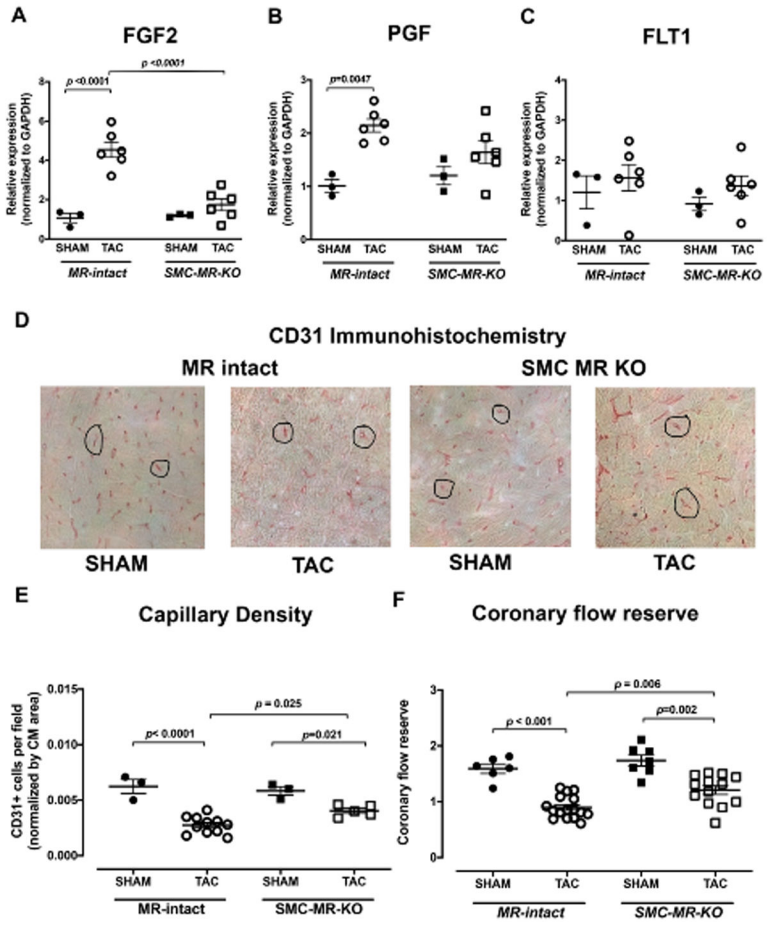

Figure 6: Deletion of mineralocorticoid receptor in smooth muscle cell (SMC-MR-KO) improves capillary density and coronary flow reserve in pressure overload-induced heart failure.

Results of quantitative RT-PCR for angiogenesis markers: **(A)** basic fibroblast growth factor (FGF2), **(B)** placental growth factor (PGF), and **(C)** vascular endothelial growth factor receptor 1 (FLT1). **(D)** Representative LV sections stained with CD31 to mark endothelial cells. Scale bar=50 μm. **(E)** Quantification of capillary density using CD31 stained area normalized to cardiomyocyte area. **(F)** Coronary flow reserve assessed by echocardiography before and after a hyperemic stimulus. A-C: MR-intact Sham n=3, MR-intact TAC n=6, SMC-MR-KO Sham n=3, SMC-MR-KO TAC n=6. E: MR-intact Sham n=3, MR-intact TAC n=11, SMC-MR-KO Sham n=3, SMC-MR-KO TAC n=5. F: MR-intact Sham n=6, MR-intact TAC n=16, SMC-MR-KO Sham n=7, SMC-MR-KO TAC n=13. Two-way ANOVA with Tukey post-hoc test.

Table 1.

Survival rate, physical characteristics, echocardiography, and pressure-volume loop analysis-derived indices:

Survival (%): the number of mice that survived out of the total number of mice that received the surgery

	MR-intact SHAM (n=9)	MR-intact TAC (n=27)	SMC-MR-KO SHAM (n=10)	SMC-MR-KO TAC (n=17)
Survival	9 / 9 (100%)	27 / 32 (84%)	10 / 10 (100%)	17 / 22 (77%)
BW (g)	26.8 ± 2.10	25.2 ± 2.08	26.1 ± 1.41	25.6 ± 1.65
KW (mg)	158.8 ± 21.30	143.1 ± 24.42	158.5 ± 11.59	155.5 ± 21.85
KW(mg):BW(g)	5.9 ± 0.60	5.7 ± 0.52	6.1 ± 0.56	6.1 ± 0.42
HW (mg)	119.0 ± 16.50	194.7 ± 33.25 *	117.0 ± 9.62	174.3 ± 21.44 *†
aPWV (mm/ms)	2.1 ± 0.30	2.4 ± 0.5196	2.2 ± 0.57	2.2 ± 0.4123
Aortic SBP (mmHg)	87.3 ± 9.30	137.9 ± 29.10 *	81.6 ± 11.88	128.7 ± 23.50 *
SV (uL)	21.7 ± 4.20	11.7 ± 3.64 *	22.7 ± 3.68	16.4 ± 4.54 *‡
CO (uL/min)	10968 ± 207.0	6178 ± 1927.7 *	10459 ± 1558.2	8682 ± 1863.6 §‡

BW: body weight; KW: kidney weight; KW:BW: kidney weight to body weight ratio; HW, whole heart weight; aPWV, aortic pulse wave velocity assessed by ultrasound; SBP: carotid systolic blood pressure obtained during PV loop analysis proximal to the aortic constriction in anesthetized mice; SV: stroke volume obtained during PV loop analysis; CO: cardiac output obtained during PV loop analysis. The values are presented as mean +/− standard deviation. Two-way ANOVA:

* $p<0.01$ versus genotype-matched SHAM mice.

† $p<0.05$ versus MR-intact TAC mice.

‡ $p<0.01$ versus MR-intact TAC mice.

§ $p<0.05$ versus genotype-matched SHAM mice.

Table 2.

The impact of systemic MR inhibition or cell-specific deletion of MR on heart failure outcomes in pressure overload-induced mouse models of heart failure.

Treatment	Model	Sex	Cardiac Hypertrophy	Cardiac Dilation	Cardiac Fibrosis	Cardiac Function	Cardiac Inflammation	Capillary Density	Coronary Flow Reserve	Reference
none	TAC (27G)	Male	↑	↑	↑	↓	↑	↓	↓	8, 24, 25, Present Study
MR inhibition (Spironolactone / Eplerenone)	TAC/AAC (27G)	Male	↓	↓	↓	↑	↓	NR	NR	12, 13, 26, 27, 28
Cell Type From Which MR Deleted										
SMC	TAC (27G)	Male	↓	↓	↓	↑	↓	↑	↑	Present study
Cardiomyocyte	TAC (27G)	Male	=	↓	=	↑	=	NR	NR	14
Fibroblast	TAC (27G)	Male	=	=	=	=	=	NR	NR	14
Endothelial	TAC (25G)	Male	=	=	=	↑	=	=	NR	15
T Cell	AAC (27G)	Male	↓	↓	↓	↑	↓	NR	NR	28
Myeloid Cell	AAC (27G)	Male	↓	NR	↓	NR	↓	NR	NR	29

TAC: transverse aortic constriction, AAC: abdominal aortic constriction, MR: mineralocorticoid receptor, NR: not reported in the manuscript, SMC: smooth muscle cell. 27G: 27 gauge needle used for pressure overload surgery.